ENGINEERING TRANSACTIONS • Engng. Trans. • 44, 3–4, 389–402, 1996
Polish Academy of Sciences • Institute of Fundamental Technological Research

WORK-HARDENING IN THREE-DIMENSIONAL SLIP-LINE FIELDS

R. L. BISH (MELBOURNE)

A slip-line field theory that includes rotational continuity, published in an earlier article and shown therein to lead to Hill's equiangular net, is extended to include work-hardening. This object is achieved by applying a rule of work-hardening shown in another earlier article to lead to the load observed in plane-strain extrusion experiments, work hardening having been shown to make a substantial contribution. The three-dimensional slip-line field theory developed in the paper is applied to the problem of a tube drawn through a conical die. It is shown how the force necessary to hold the tube against the die and so to prevent wrinkling may be calculated.

1. Introduction

In an earlier paper [1], the author presented a three-dimensional slip-line field theory that could be applied to the ideal solid. The theory relies on a principle concerned with the rotations of the crystal-grains within the plastically deforming body, since with plastic deformation the grains rotate to bring about a state of crystallographic alignment with respect to the maximum shear surfaces. In precise terms this principle states that, if to a fully textured, ductile, polycrystalline body forces are applied of such a nature as to cause plastic flow, then the crystal-grains within the plastically deforming region of that body will rotate in such a way as to present their planes of crystallographic slip parallel to the surfaces of maximum shear stress and will continue to do so as long as the deformation is continued. This paper presents a further development of the theory in which work-hardening is included.

In order to properly describe work-hardening in a three-dimensional slip-line field we need to note the fact that rotation of a crystal-grain within a plastically deforming fully textured polycrystalline body takes place by slip occurring on two intersecting families of crystallographic planes within that grain, the angle of rotation of the grain as a whole equalling the angles of rotation of its individual rigid parts. Since rotation demands double-slip, which is also essential for work-hardening [2], we may state [3, 4] a second principle:

when a fully textured, ductile, polycrystalline body is plastically deformed in any manner, work-hardening occurs due to the internal re-alignments alone that accompany the external shape changes. The words, in any manner, need to be emphasised because we may apply this principle in the interpretation of uniaxial tensile test data so that analysis may then be made of such diverse metal working processes as drawing and cold-forging.

It follows from the two principles stated that in any fully textured polycrystalline solid, yielding will commence when the greatest of the three maximum shear stresses in the body reaches a critical level depending upon prior cold-work. This is, of course, Tresca's yield criterion, which must apply to the body under consideration because the physical and mathematical maximum shear surfaces remain mutually aligned and because the former are enveloped by planes (within each intersected crystal-grain) of crystallographic slip. A flow rule also follows immediately from the first of the above two principles but we shall see that, by commencing with PRAGERS flow rule [5], the Tresca yield criterion becomes identical, for the solids that we are considering, to the von Mises yield condition.

These principles, together with the stress-equilibrium equations, form the basis of the three-dimensional slip-line field theory for work-hardening solids now to be presented.

2. The three-dimensional slip-line net

The yield cylinder associated with Tresca's yield criterion is shown in stress-space in Fig. 1a, where σ_1, σ_2, σ_3 are the three principal stresses associated with the stress-tensor σ_{ij}. The sides A and B of this cylinder have normals that are perpendicular to the σ_3-axis, and a section through the yield cylinder normal to the σ_3-axis is shown in Fig. 1b. By Prager's flow rule, when the stress-point lies on either A or B in Fig. 1a, if $\dot{\varepsilon}_{ij}$ denotes the strain-rate tensor, $\dot{\varepsilon}_3$ equals zero. Likewise the sides C and D have normals perpendicular to the σ_2-axis and when the stress-point lies on either of these sides of the cylinder, $\dot{\varepsilon}_2$ equals zero. When the stress-point lies on E or F in Fig. 1a, these sides being parallel to the σ_1-axis, $\dot{\varepsilon}_1$ vanishes. The cases where the stress-point lies on an edge of the yield cylinder are included in this description since, as KOITER [6] points out, the stress-point must always be stationed so that the normal to the yield surface remains definite. Consequently, as shown in Figs. 1c, 1 d and 1 e, the slip-line net can only have one of three possible configurations. In each case the net is confined to a family of parallel surfaces of principal stress within the deforming body normal to

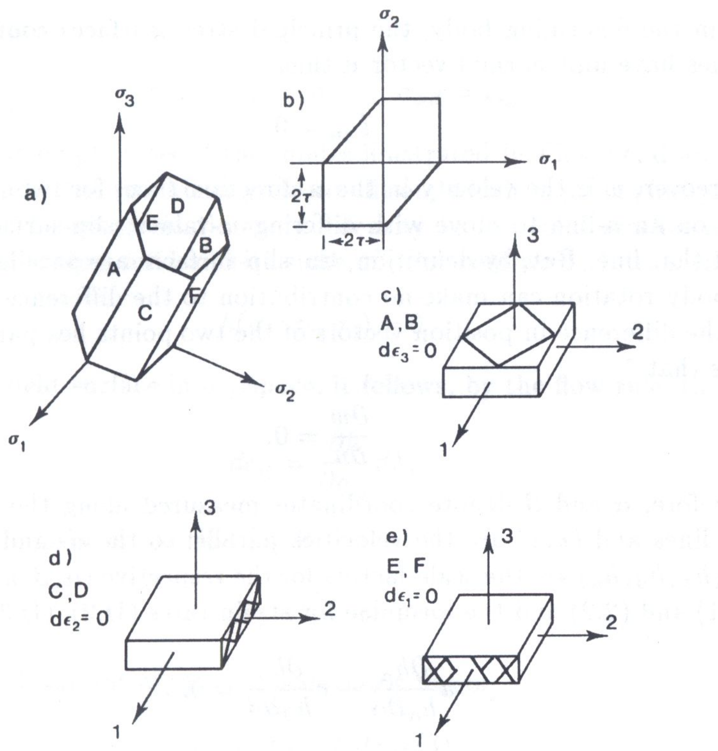

FIG. 1.

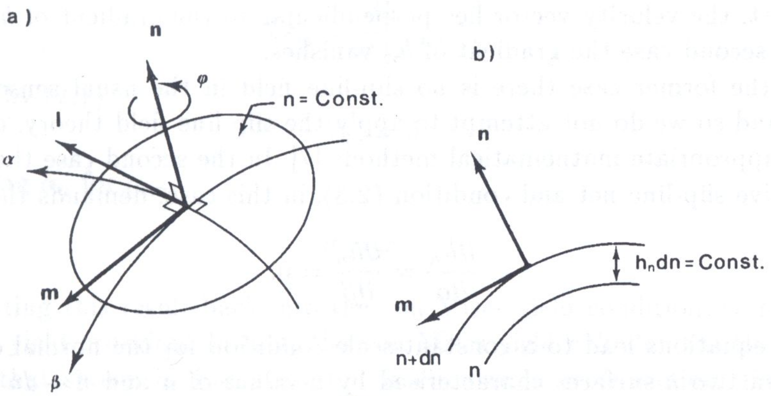

FIG. 2.

which the strain-rate vanishes (Fig. 2a). Within this three-dimensional net we define a slip-line as a curve in space along which a surface of principal stress, on which the yield criteria are satisfied, is intersected by a member of one of the two families of orthogonal surfaces of maximum shear stress associated with that principal stress surface.

If, in the deforming body, the principal stress surfaces containing these slip-lines have unit normal vector **n** then

$$\dot{\varepsilon}_{nn} = 0. \tag{2.1}$$

If, moreover, w is the velocity in the **n**-direction then, for two neighbouring points on an n-line to move with differing w-values, slip-surfaces must intersect that line. But, by definition, the slip-surfaces are parallel to **n**, while rigid-body rotation can make no contribution to the difference in w-values, since the difference in position vectors of the two points lies parallel to **n**. It follows that

$$\frac{\partial w}{\partial n} = 0. \tag{2.2}$$

If therefore, α and β denote coordinates measured along the two families of slip-lines and (u, v) are the velocities parallel to the α- and β-slip-lines, while (h_α, h_β, h_n) are the scale-factors for the respective (α, β, n)-lines, then, by (2.1) and (2.2) and the formulae for strain rates (D.2), (D.3) in [1]

$$u\frac{\partial h_n}{h_\alpha \partial \alpha} + v\frac{\partial h_n}{h_\beta \partial \beta} = 0. \tag{2.3}$$

In the notation of Fig. 2a the left-hand member in this equation equals $(u_{\mathrm{l}} + v_{\mathrm{m}})\cdot\mathrm{grad}\, h_n$ and there are only two ways in which (2.3) can be satisfied. In the first, the velocity vector lies perpendicular to the gradient of h_n, while in the second case the gradient of h_n vanishes.

In the former case there is no slip-line field in the usual sense of this term and so we do not attempt to apply the slip-line field theory, choosing more appropriate mathematical methods [7]. In the second case there is an extensive slip-line net and condition (2.3), in this case, demands that

$$\frac{\partial h_n}{\partial \alpha} = \frac{\partial h_n}{\partial \beta} = 0. \tag{2.4}$$

These equations lead to a constant-scale condition for the normal distance between two n-surfaces characterised by n-values of n and $n + dn$ is $h_n dn$ and, by (2.4), this is constant over those surfaces (Fig. 2b); it is a necessary condition for slip in the case of elements such as that shown in Fig. 1c.

There are also simplifications that can be introduced simply because the net lies on a surface of principal stress, while the slip-lines on it lie parallel to surfaces of the maximum shear stress. Thus

$$\sigma_{n\alpha} = \sigma_{n\beta} = 0, \tag{2.5}$$

while we write

$$\sigma_{\alpha\alpha} = \sigma_{\beta\beta} = \sigma, \qquad \sigma_{\alpha\beta} = \tau. \tag{2.6}$$

We may attempt to see if the modes illustrated in Figs. 1 c, d and e are also governed by the von Mises yield condition, which requires that yielding occurs when the shear elastic energy density in the solid reaches a value characteristic of that solid and its state of prior cold-work. In this case, if

$$h(\sigma_1, \sigma_2, \sigma_3) = 0$$

denotes the yield surface in σ_{ij}-space, it follows, by the flow rule, that

$$d\varepsilon_{ij} = \frac{\partial h}{\partial \sigma_{ij}} d\lambda,$$

where λ is a multiplier, so that [8], if

$$J_2 = \frac{1}{2}\tau_{ij}\tau_{ij}\,,$$

is the second invariant of the stress-deviator tensor

$$\tau_{ij} = \sigma_{ij} - \delta_{ij}(\sigma_{\ell\ell}/3)$$

then,

$$d\varepsilon_{ij} = \frac{\partial h}{\partial J_2}\tau_{ij} d\lambda,$$

so that, by (2.1),

$$\tau_{nn} = 0$$

or, writing σ_n for σ_{nn},

$$\sigma = \sigma_n\,. \tag{2.7}$$

Substituting this result back into the von Mises yield condition we recover Tresca's yield criterion. In fact, the von Mises yield cylinder has the same axis as that shown in Fig. 1 a but it is circular in cross-section, Eq. (2.1) being true along six of its generators.

3. The equation of work-hardening

Let us consider a process wherein the solid is unloaded from the plastic state and is then reloaded to yield along a new path, so that all the elements of the body, within the new deforming region, must rotate in order to align themselves crystallographically with the new surfaces of maximum shear stress; a process during which the solid suffers no external shape changes of plastic order.

If

$$\boldsymbol{\omega} = \dot{\phi}\,\mathbf{n}$$

is the rotation/rate vector of an element of the body and $\dot{\mathbf{e}}$ is the velocity, due to the rotation, we have for two neighbouring points with position vectors $\mathbf{r}$ and $\mathbf{r} + d\mathbf{r}$

$$d\dot{\mathbf{e}} + \boldsymbol{\omega} \times d\mathbf{r} = 0. \tag{3.1}$$

On the other hand,

$$\mathbf{l} \cdot (\boldsymbol{\omega} \times d\mathbf{r}) = \dot{\phi}\mathbf{n} \cdot (d\mathbf{r} \times \mathbf{l}) = -\dot{\phi} h_\beta \, d\beta,$$
$$\mathbf{m} \cdot (\boldsymbol{\omega} \times d\mathbf{r}) = \dot{\phi}\mathbf{n} \cdot (d\mathbf{r} \times \mathbf{m}) = \dot{\phi} h_\alpha \, d\alpha,$$

since $h_\alpha d\alpha$ and $h_\beta d\beta$ are merely the components of dr resolved along the respective α- and β-lines. Thus (3.1), resolved into its α- and β-component equations, becomes

$$\mathbf{l} \cdot d\dot{\mathbf{e}} - \dot{\phi} h_\beta \, d\beta = 0,$$
$$\mathbf{m} \cdot d\dot{\mathbf{e}} + \dot{\phi} h_\alpha \, d\alpha = 0.$$

The maximum shear strain rate, $\dot{\gamma}$, equals the coefficient of $h_\alpha d\alpha$ in $\mathbf{m} \cdot d\dot{\mathbf{e}}$ or of $h_\beta d\beta$ in $\mathbf{l} \cdot d\dot{\mathbf{e}}$ so that, from the above two equations, during re-alignment, $\dot{\gamma}$ equals $-\dot{\phi}$ along the α-lines or $+\dot{\phi}$ along the β-lines. The signs are consistent with a sign convention that applies to ϕ. By the second principle of Sec. 1 it follows that the shear-stress/shear-strain relation

$$\tau = \tau(\gamma)$$

for the solid may be re-expressed in the form

$$\tau = \tau(\phi), \tag{3.2}$$

provided, of course, that the reference direction for ϕ is suitably defined. Now we see that the relation between stress and strain, obtained by loading a standard test-piece of the material, may be re-interpreted in such a way as to provide the relation between the maximum shear stress and the net angle within the deforming solid. We must now consider the equation governing ϕ itself.

4. The harmonic nature of ϕ

If $\boldsymbol{\omega}$ denotes the rotation-rate vector at any point in the solid, the spatial continuation of $\boldsymbol{\omega}$, which follows immediately from our first principle, demands that

$$\operatorname{curl}\boldsymbol{\omega} = 0.$$

From this equation and the following formulae, where $\mathbf{v}$ is the velocity,

$$\dot{\boldsymbol{\varepsilon}} = \frac{1}{2}\left\{\operatorname{grad}\mathbf{v} + (\operatorname{grad}\mathbf{v})^T\right\},$$
$$\operatorname{div}\mathbf{v} = 0,$$
$$\boldsymbol{\omega} = \frac{1}{2}\operatorname{curl}\mathbf{v},$$

we obtain

(4.1) $$\operatorname{div}\dot{\boldsymbol{\varepsilon}} = 0.$$

Moreover

$$\dot{\varepsilon}_{n\alpha} = \dot{\varepsilon}_{n\beta} = 0,$$

and since

$$\dot{\varepsilon}_{\alpha\alpha} = \dot{\varepsilon}_{\beta\beta} = 0,$$

we obtain, from (4.1), by analogy with the stress-equilibrium equations (A.1), (A.2) in [1] or otherwise,

$$\frac{2\dot{\gamma}}{h_\alpha}\frac{\partial h_\alpha}{\partial\beta} + \frac{\partial\dot{\gamma}}{\partial\beta} = 0,$$
$$\frac{2\dot{\gamma}}{h_\beta}\frac{\partial h_\beta}{\partial\alpha} + \frac{\partial\dot{\gamma}}{\partial\alpha} = 0.$$

From these equations we obtain

$$\frac{\partial}{\partial\alpha}\left(\frac{1}{h_\alpha}\frac{\partial h_\alpha}{\partial\beta}\right) = \frac{\partial}{\partial\beta}\left(\frac{1}{h_\beta}\frac{\partial h_\beta}{\partial\alpha}\right)$$

or, on substituting for the derivatives of h_α, h_β (B.11), (B.12) in [1]

(4.2) $$\frac{\partial}{\partial\alpha}\left(\frac{h_\beta}{h_\alpha}\frac{\partial\phi}{\partial\alpha}\right) + \frac{\partial}{\partial\beta}\left(\frac{h_\alpha}{h_\beta}\frac{\partial\phi}{\partial\beta}\right) = 0.$$

But $\mathbf{n}$ is measured along a principal stress axis, while ϕ is a physical rotation, so that it necessarily follows, since torsion about $\mathbf{n}$ would imply shear stresses on planes containing the n-direction, that

(4.3) $$\frac{\partial\phi}{\partial n} = 0.$$

From (2.4), (4.2) and (4.3) we thus obtain, by the formula (B.15) in [1] for the three-dimensional Laplace equation,

$$\nabla^2\phi = 0. \tag{4.4}$$

5. Stress-Equilibrium

On substituting from (2.4)–(2.7) into the stress-equilibrium equations (A.1)–(A.3) in [1] we obtain, using the formulae for the derivatives of h_α, h_β (B.11), (B.12) in [1]

$$\frac{\partial\sigma}{h_\alpha\partial\alpha} - 2\tau\frac{\partial\phi}{h_\alpha\partial\alpha} + \frac{\partial\tau}{h_\beta\partial\beta} = 0, \tag{5.1}$$

$$\frac{\partial\sigma}{h_\beta\partial\beta} + 2\tau\frac{\partial\phi}{h_\beta\partial\beta} + \frac{\partial\tau}{h_\alpha\partial\alpha} = 0, \tag{5.2}$$

$$\frac{\partial\sigma}{\partial n} = 0. \tag{5.3}$$

But, by (3.2),

$$\frac{\partial\tau}{\partial\alpha} = \frac{d\tau}{d\phi}\frac{\partial\phi}{\partial\alpha}, \qquad \frac{\partial\tau}{\partial\beta} = \frac{d\tau}{d\phi}\frac{\partial\phi}{\partial\beta},$$

while, by (4.3) and (5.3), $\sigma = \sigma(\phi)$, so that

$$\frac{\partial\sigma}{\partial\alpha} = \frac{d\sigma}{d\phi}\frac{\partial\phi}{\partial\alpha}, \qquad \frac{\partial\sigma}{\partial\beta} = \frac{d\sigma}{d\phi}\frac{\partial\phi}{\partial\beta}.$$

With these equations, (5.1) and (5.2) may be re-expressed in the matrix form

$$\begin{bmatrix} d\sigma - 2\tau\, d\phi & d\tau \\ d\tau & d\sigma + 2\tau d\phi \end{bmatrix} \begin{bmatrix} \dfrac{\partial\phi}{h_\alpha\partial\alpha} \\ \dfrac{\partial\phi}{h_\beta\partial\beta} \end{bmatrix} = \begin{bmatrix} 0 \\ 0 \end{bmatrix},$$

for which the consistency condition is

$$\begin{vmatrix} d\sigma - 2\tau d\phi & d\tau \\ d\tau & d\sigma + 2\tau d\phi \end{vmatrix} = 0,$$

or

$$d\sigma^2 = d\tau^2 + 4\tau^2 d\phi^2. \tag{5.4}$$

This is the first order equation governing σ and τ.

On the other hand, on multiplying (5.1) by h_α and differentiating with respect to β, we obtain

$$\frac{\partial^2\sigma}{\partial\alpha\partial\beta} - 2\tau\frac{\partial^2\phi}{\partial\alpha\partial\beta} - 2\frac{\partial\tau}{\partial\beta}\frac{\partial\phi}{\partial\alpha} + \frac{\partial}{\partial\beta}\left(\frac{h_\alpha}{h_\beta}\frac{\partial\tau}{\partial\beta}\right) = 0 \tag{5.5}$$

while, in a similar fashion from (5.2), we get

$$\frac{\partial^2\sigma}{\partial\alpha\partial\beta} + 2\tau\frac{\partial^2\phi}{\partial\alpha\partial\beta} + 2\frac{\partial\tau}{\partial\alpha}\frac{\partial\phi}{\partial\beta} + \frac{\partial}{\partial\alpha}\left(\frac{h_\beta}{h_\alpha}\frac{\partial\tau}{\partial\alpha}\right) = 0. \tag{5.6}$$

From (3.2)

$$\frac{\partial\tau}{\partial\alpha}\frac{\partial\phi}{\partial\beta} - \frac{\partial\tau}{\partial\beta}\frac{\partial\phi}{\partial\alpha} = 0, \tag{5.7}$$

while, by (3.2) and (4.3),

$$\frac{\partial\tau}{\partial n} = 0. \tag{5.8}$$

Adding (5.5) and (5.6) and using (5.7) with (2.4) and (5.8) and the formula (B.15) in [1] for the Laplacian in three-dimensions we obtain

$$2\frac{\partial^2\sigma}{\partial\alpha\partial\beta} + h_\alpha h_\beta\nabla^2\tau = 0, \tag{5.9}$$

which is the second order partial differential equation governing σ and τ.

6. Application to tube drawing

Figure 3 serves to illustrate a simple solution to (4.4) that describes slip-lines on a principal stress surface that is of conical form. The expression for ϕ on any one of these cones is

$$\phi = \ln(a/r), \tag{6.1}$$

the principal stress surfaces themselves being given by

$$r + (z - c)\tan \mathbf{A} = b,$$

where (r, z) are the usual cylindrical coordinates measured from an origin located at the centre of the base of the cone, A being the semi-apex angle of each cone, c equalling a constant characterising the particular cone concerned, while b is a further constant. Shown in Fig. 3 b is the field obtained for $A = \pi/2$ $(z = c)$, while illustrated in Fig. 3 c is the field for $A = 0$ $(r = b)$.

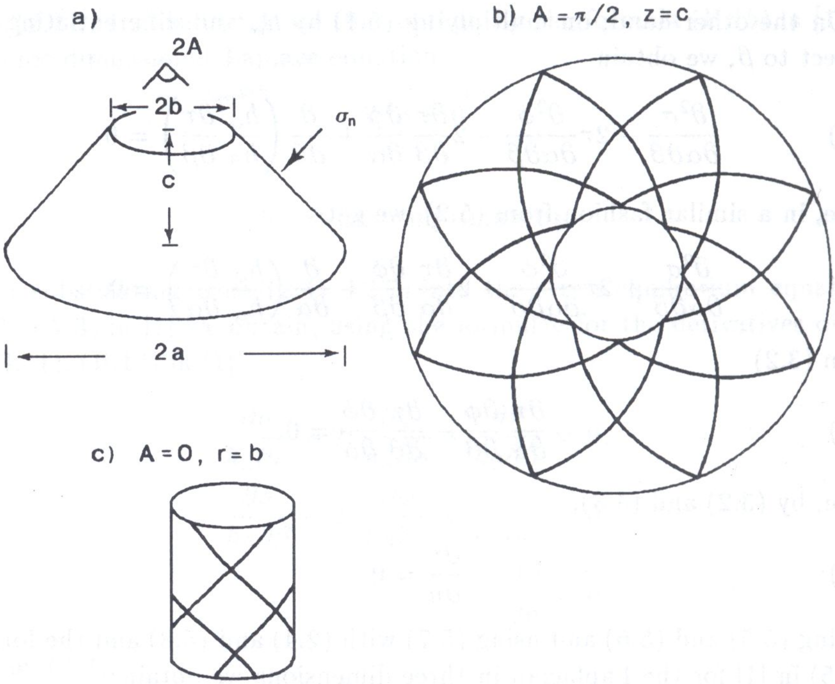

FIG. 3.

We may apply the field shown in Fig. 3 in solving the problem of a tube drawn through a conical die, the tube being subjected in the process to a reduction in diameter. Of course, the tube will wrinkle circumferentially unless supported from the inside. The problem is to calculate the normal stress, σ_n, on a cone-shaped mandrel serving to support the tube; the die and mandrel surfaces are assumed to be smooth.

For the slip-line field illustrated in Fig. 3 a we obtain, from (5.4), on integrating along an α-line and letting σ_0 and τ_0 represent the values of σ and τ at the wider end of the tube, writing τ' for $d\tau/d\gamma$ at $\gamma = \phi$ on the stress-strain curve for the solid, the result

$$\sigma = \sigma_0 + \int_0^{\ln(a/r)} \sqrt{(\tau')^2 + 4\tau^2}\, d\phi,$$

$$\sigma_0 + \tau_0 = 0$$

so that, by (2.7),

$$\sigma_n = -\tau_0 + \int_0^{\ln(a/r)} \sqrt{(\tau')^2 + 4\tau^2}\, d\phi. \tag{6.2}$$

It is important to note that in choosing the lower limit of integration in this formula equal to zero it has, in fact, been assumed that the tube has been cold-worked in a previous operation leaving slip-lines of the form shown in Fig. 3 c. When the tube has been fully cold-worked in this prior operation, so that $\tau' = 0$, Eq. (6.2) becomes, for the drawing of the tube through a conical die,

$$\sigma_n = -\tau_\infty \Big\{ 1 + 2 \ln(a/r) \Big\}, \tag{6.3}$$

where τ_∞ is the shear yield stress of the material in its fully work-hardened condition.

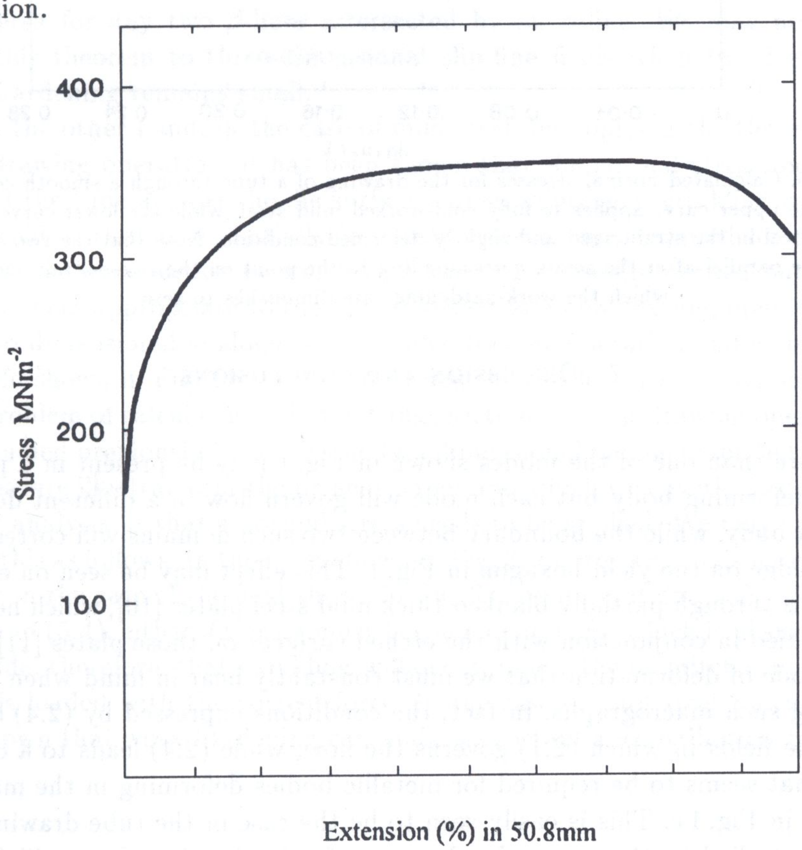

FIG. 4. Stress-strain curve for mild steel; strain-aged and slightly deformed.

By integrating and resolving the stress parallel to the axis we may determine, from these formulae, the forces that need to be applied to a mandrel located inside the tube, to prevent it from wrinkling. Results of computations of σ_n, using tensile-test data for mild steel [9] (Fig. 4), are shown in Fig. 5.

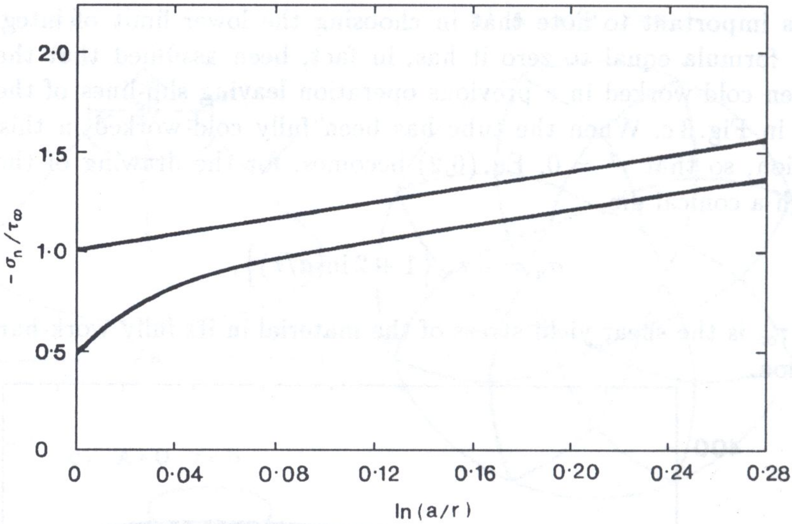

FIG. 5. Calculated normal stresses for the drawing of a tube through a smooth conical die; the upper curve applies to fully cold-worked mild steel, while the lower curve is for mild steel in the strain-aged and slightly deformed condition. Note that the two curves become parallel after the strain corresponding to the point on the stress-strain curve at which the work-hardening rate diminishes to zero.

7. Discussion and conclusions

More than one of the modes shown in Fig. 1 may be present in a plastically deforming body but each mode will govern flow in a different domain of that body, while the boundary between two such domains will correspond to an edge on the yield hexagon in Fig. 1. This effect may be seen on etched sections through partially blanked thick mild steel plates [10], which need to be studied in conjunction with the etched surfaces on those plates [11]. It is the mode of deformation that we must constantly bear in mind when interpreting such macrographs. In fact, the conditions expressed by (2.4) define slip-line fields in which (2.1) governs the flow, while (2.4) leads to a condition that seems to be required for metallic bodies deforming in the manner shown in Fig. 1 c. This is easily seen to be the case in the tube-drawing example studied in the paper. In the case of tube-drawing there will be, in addition to the field shown in Fig. 3 a, small transition zones at the forward and rear ends of the frustum-shaped region of the tube. In these transition regions the mode is that of Figs. 1 d or 1 e.

Work-hardening has been included in the three-dimensional theory described and this has been achieved by extending a hypothesis proposed in earlier papers; in the case of extrusion through a lubricated wedge-shaped die having two-dimensional symmetry, this hypothesis led to a predicted load in very close agreement with that observed [12]. Most cold-worked metals and alloys, moreover, work-harden to only a small degree and with these metals the plastic limb on the stress-strain curve is almost linear. In these cases the second term in the left-hand member of (5.9) vanishes by (4.4), so that the same equation that governs σ, as in the theory for the ideal solid, also governs σ in the case of a solid that work-hardens to a slight degree. In the two-dimensional case this result leads to the corollary to Hencky's first theorem for σ, which states that along any two α-lines the difference in σ, where those lines are intersected by a β-line, remains constant, and vice-versa for any two β-lines intersected by an α-line. We may now extend this theorem to three-dimensional slip-line fields when the degree of work-hardening remains small.

On the other hand, in the case of mild steel, by applying the theory to a tube-drawing operation, it has been shown that the normal stress required to hold the tube against the die surface and so to prevent wrinkling is, for a prior cold-worked tube, initially in excess of twice that required for a tube of steel in the condition in which cold-forming is usually carried out. The slip-line field appropriate to the flange section in a cup-drawing operation is the two-dimensional analogue of this tube drawing operation and is, in fact, the field shown in Fig. 3 b (in the case when the cup has circular symmetry). The problem of calculating σ in the flange section in a cup-drawing operation was studied previously [4], using the two-dimensional and incomplete theory. The feature illustrated in the present paper and which was overlooked in the earlier analysis, is that a normal stress needs to be applied. We may, in fact, prove this as follows. In the cases shown in Fig. 3, a normal stress is necessary, except in the case of the field shown in Fig. 3 c, because, if $d\sigma_n = 0$, then, by (2.7) and (5.4), either $d\phi$ or $d\tau$ must become imaginary, which is absurd. We conclude, therefore, that wrinkling will occur, unless the mandrel or pressure plate is loaded with the correct force. In the case of mild steel, calculation has shown that work-hardening can make a substantial contribution to that force.

References

1. R.L. Bish, *Three-dimensional slip-line field theory with rotational continuity*, Engng. Trans., **44**, 2, 207–228, 1996.
2. E.R. Parker, *Modern concepts of flow and fracture*, Edward De Mille Campbell Memorial Lecture (ASM), **50**, 52–104, 1957.
3. R.L. Bish, *The flow of a work-hardening solid by inviscid slip between elastic domains*, Acta Mech., **83**, 1–7, 1990.

4. R.L. BISH, *Plane-stress deformation of a flat plate by slip between elastic elements*, Arch. Mech., **46**, 1, 3–12, 1994.
5. W. PRAGER, *Recent developments in plasticity*, J. Appl. Phys., **20**, 235–241, 1949.
6. W.T. KOITER, *Stress-strain relations, uniqueness and variational theorems for elastic-plastic materials with a singular yield surface*, Quart. Appl. Math., **11**, 350–354, 1953.
7. R.L. BISH, *Transverse deflection of a cold-worked metal plate clamped around its edge*, Engng. Trans., **43**, 4, 627–635, 1995.
8. P. PERZYNA, *The constitutive equations for rate-sensitive plastic materials*, Quart. Appl. Math., **20**, 321–332, 1963.
9. J.D. JEVONS, *The metallurgy of deep drawing and pressing*, Chapman & Hall, 1941.
10. L.E. SAMUELS, *Optical microscopy of carbon steels*, ASM, 1980.
11. R.L. BISH, *Etching of plastic zones in mild steel*, J. Aust. Inst. of Metals, **21**, 167–168, 1976.
12. R.L. BISH, *The plane-strain extrusion of a work-hardening solid*, Acta Mech., **85**, 125–130, 1990.

AERONAUTICAL AND MARITIME RESEARCH LABORATORY
MELBOURNE, AUSTRALIA.

Received May 9, 1996.